Synthesis, Electrochemistry and X-Ray Crystal Structure of *cis*-$[Ru^{III}L^1(Cl)(H_2O)][ClO_4]_2\cdot 2H_2O$ [L^1 = *N,N'*-dimethyl-*N,N'*-bis(2-pyridylmethyl)ethylenediamine];† Electrochemical Oxidation of Alcohols and Tetrahydrofuran by *cis*-$[Ru^VL^1(Cl)O]^{2+}$

Chi-Keung Li,[a] Wai-Tong Tang,[a] Chi-Ming Che,*[,a] Kwok-Yin Wong,[b] Ru-Ji Wang[c] and Thomas C. W. Mak[c]
[a] *Department of Chemistry, University of Hong Kong, Pokfulum Road, Hong Kong*
[b] *Department of Applied Biology and Chemical Technology, Hong Kong Polytechnic, Hunghom, Kowloon, Hong Kong*
[c] *Department of Chemistry, The Chinese University of Hong Kong, Shatin, New Territories, Hong Kong*

Reaction of $K_2[RuCl_5(H_2O)]$ with *N,N'*-dimethyl-*N,N'*-bis(2-pyridylmethyl)ethylenediamine (L^1) in ethanol gave *cis*-$[Ru^{III}L^1Cl_2]^+$ and then *cis*-$[Ru^{III}L^1(Cl)(H_2O)]^{2+}$ upon reaction with Ag^I in water. The structure of *cis*-$[Ru^{III}L^1(Cl)(H_2O)][ClO_4]_2\cdot 2H_2O$ has been established by X-ray crystallography: space group *Pbca*, $a = 10.863(1)$, $b = 21.548(2)$, $c = 21.912(2)$ Å. The measured Ru–Cl and Ru–OH_2 distances are 2.307(4) Å and 2.070(9) Å respectively. A cyclic voltammogram of *cis*- $[Ru^{III}L^1(Cl)(H_2O)]^{2+}$ in 0.1 mol dm^{-3} CF_3CO_2H shows three reversible/quasi-reversible couples at 1.29, 0.93 and 0.23 V *vs.* saturated calomel electrode assigned to the couples Ru^V–Ru^{IV}, Ru^{IV}–Ru^{III} and Ru^{III}–Ru^{II}. The complex *cis*-$[Ru^{III}L^1(Cl)(H_2O)]^{2+}$ is an active catalyst for the electrochemical oxidation of alcohols and tetrahydrofuran. The second-order rate constant for the oxidation of benzyl alcohol by electrochemically generated *cis*-$[Ru^VL^1(Cl)O]^{2+}$ is estimated to be 8.4×10^4 dm^3 mol^{-1} s^{-1}.

Ruthenium oxo complexes are of current interest because of their remarkable abilities in stoichiometric and catalytic oxidation of organic substrates.[1] In this context, complexes having the Ru^V=O moiety are of particular interest because they have been suggested to play a key role in water oxidation.[2] However, such species are usually very reactive and hence difficult to isolate. Only few studies on this class of compounds have been reported.[3,4]

Multidentate chelating tertiary amines are known to stabilise high-valent Ru=O complexes.[5] In this work, the ligand *N,N'*-dimethyl-*N,N'*-bis(2-pyridylmethyl)ethylenediamine (L^1), owing to its small cavity size upon co-ordination to a metal ion, was initially chosen to generate ruthenium complexes having a *cis*-dioxo unit. However, attempts to prepare *cis*-$[Ru^{III}L^1(OH)(H_2O)]^{2+}$ led to isolation of the stable *cis*- $[Ru^{III}L^1(Cl)(H_2O)]^{2+}$, which can be easily oxidised to *cis*-$[Ru^VL^1(Cl)O]^{2+}$ by electrochemical means.

Experimental

The salt $K_2[RuCl_5(H_2O)]$ was purchased from Johnson Matthey Ltd. Water was distilled twice from potassium permanganate and trifluoroacetic acid was distilled under nitrogen. All solvents and organic substrates were purified by repeated recrystallisation or distillation. The ligand L^1 was synthesised from pyridine-2-carbaldehyde and 1,2-diaminoethane.[6]

cis-$[Ru^{III}L^1Cl_2]ClO_4$.—An ethanolic solution of L^1 (0.5 g, in 200 cm^3) was added dropwise to a stirred ethanolic suspension of $K_2[RuCl_5(H_2O)]$ (0.5 g, in 250 cm^3) heated under reflux. The addition process took about 3 h for completion and the mixture was then refluxed for 1 d. It was filtered and the filtrate, with a few drops of concentrated HCl, was evaporated to dryness to give crude *cis*-$[Ru^{III}L^1Cl_2]Cl$. The perchlorate salt was obtained by metathesis with $NaClO_4$ in dilute hydrochloric acid (2 mol dm^{-3}). Pure samples could be recrystallised from hot HCl (60 °C, 2 mol dm^{-3}), yield 60%. UV-VIS in MeCN [λ_{max}/nm (ε_{max}/dm^3 mol^{-1} cm^{-1})]: 409 (2360) and 297 (5590) (Found: C, 36.8; H, 4.3; Cl, 19.0; N, 10.1. Calc. for *cis*-$[Ru^{III}L^1Cl_2]ClO_4$: C, 36.9; H, 4.3; Cl, 18.9; N, 10.2%).

cis-$[Ru^{III}L^1(Cl)(H_2O)][ClO_4]_2\cdot 2H_2O$.—A mixture of *cis*-$[Ru^{III}L^1Cl_2]ClO_4$ (0.3 g) and silver(I) toluene-*p*-sulphonate (0.5 g) in distilled water (10 cm^3) was heated at 80 °C for 1 h. The insoluble AgCl was filtered off, giving a greenish yellow solution. Greenish yellow *cis*-$[Ru^{III}L^1(Cl)(H_2O)][ClO_4]_2\cdot 2H_2O$ was precipitated on addition of $NaClO_4$. The crude product was recrystallised from aqueous trifluoroacetic acid (0.1 mol dm^{-3}). λ_{max}/nm (ε_{max}/ dm^3 mol^{-1} cm^{-1}): 355 (1570) and 268 (7140). μ_{eff} (solid sample, Guoy method) 1.80 μ_B at 300 K.

CAUTION: perchlorate salts are potentially explosive and should be handled in small quantities.

Instrumentation and Techniques.—Elemental analyses of the newly prepared compounds were performed by Butterworth Laboratories Ltd. The UV-VIS spectra were measured with a Shimadzu UV240 spectrophotometer. Magnetic susceptibilities were determined by the Guoy method with $Hg[Co(SCN)_4]$ as the calibrant. The pK_a value was determined by a spectrophotometric method at 268 and 305 nm.

---

† *cis*-Aquachloro[*N,N'*-dimethyl-*N,N'*-bis(2-pyridyl-κ*N*-methyl)ethylenediamine-κ^2*N,N'*]ruthenium(III) diperchlorate dihydrate.

Supplementary data available: see Instructions for Authors, *J. Chem. Soc., Dalton Trans.*, 1991, Issue 1, pp. xviii–xxii.

Table 1 Data collection and processing parameters for $[RuL^1Cl(H_2O)][ClO_4]_2\cdot 2H_2O$

M	659.90
a/Å	10.863(1)
b/Å	21.548(2)
c/Å	21.912(2)
U/Å^3	5129.0(8)
Z	8
$F(000)$	2680
D_c/g cm^{-3}	1.709
Space group	*Pbca* (no. 61)
Radiation	Graphite-monochromatized Mo-Kα, $\lambda = 0.710\,73$ Å
Standard reflections	302, 004
Intensity variation (%)	±1
μ/cm^{-1}	9.70
Crystal size/mm	0.16 × 0.24 × 0.28
Transmission factor range	0.724–0.790
Scan type and rate/° min^{-1}	ω, 3.01–15.63
Scan range	0.60° below Kα_1 to 0.70° above Kα_2
Background counting	Stationary counts for one-fifth of scan time at each end of scan range
Collection range	h, k, l; $2\theta_{max} = 55°$
Unique data measured	5840
Obs. data n with $\lvert F_o\rvert \geqslant 6\sigma(\lvert F_o\rvert)$	2239
No. of variables, p	277
$R = \Sigma\lVert F_o\rvert - \lvert F_c\rVert/\Sigma\lvert F_o\rvert$	0.072
Weighting scheme	$w = [1-\exp(-8\sin^2\theta/\lambda^2)][\sigma^2(F_o) + 0.0006\lvert F_o\rvert^2]^{-1}$
$R_G = [\Sigma w(\lvert F_o\rvert - \lvert F_c\rvert)^2/\Sigma w\lvert F_o\rvert^2]^{\frac{1}{2}}$	0.088
$S = [\Sigma w(\lvert F_o\rvert - \lvert F_c\rvert)^2/(n - p)]^{\frac{1}{2}}$	1.588
Residual extrema in final difference map (e Å^{-3})	+1.54 to −0.67

Table 2 Atomic coordinates ($\times 10^5$ for Ru, $\times 10^4$ for other atoms)

Atom	x	y	z
Ru	74 462(10)	11 955(4)	35 910(4)
Cl(1)	7 174(3)	1 309(2)	2 553(2)
O(1)	6 218(9)	1 899(4)	3 794(5)
N(1)	6 143(10)	480(5)	3 546(5)
N(2)	8 601(9)	425(5)	3 480(5)
N(3)	7 902(9)	1 117(5)	4 531(5)
N(4)	8 801(9)	1 875(5)	3 675(5)
C(1)	4 969(12)	508(6)	3 693(6)
C(2)	4 205(13)	14(7)	3 636(7)
C(3)	4 626(15)	−531(7)	3 421(6)
C(4)	5 867(15)	−575(7)	3 252(7)
C(5)	6 586(11)	−62(6)	3 323(7)
C(6)	7 917(12)	−33(6)	3 119(7)
C(7)	8 798(14)	155(7)	4 109(7)
C(8)	8 964(14)	705(6)	4 567(7)
C(9)	8 293(15)	1 761(7)	4 729(7)
C(10)	9 089(12)	2 043(7)	4 243(7)
C(11)	9 941(13)	2 495(7)	4 369(8)
C(12)	10 599(17)	2 747(8)	3 904(9)
C(13)	10 335(14)	2 580(7)	3 305(8)
C(14)	9 429(14)	2 129(6)	3 200(7)
C(15)	9 803(12)	562(7)	3 183(7)
C(16)	6 880(13)	891(7)	4 913(6)
Cl(2)	8 795(3)	1 285(2)	6 677(2)
O(2)	8 616(28)	755(14)	6 368(12)
O(3)	7 901(21)	1 438(10)	7 089(10)
O(4)	8 710(19)	1 708(10)	6 224(9)
O(5)	9 932(13)	1 308(6)	6 981(6)
Cl(3)	2 511(4)	1 209(2)	4 830(2)
O(6)	3 213(30)	1 737(14)	4 787(16)
O(7)	2 135(21)	1 175(9)	4 203(12)
O(8)	3 447(22)	873(11)	5 104(11)
O(9)	1 550(19)	1 332(8)	5 231(9)
O(10)	3 941(11)	1 999(6)	3 420(6)
O(11)	6 945(12)	3 051(5)	3 631(6)

Cyclic voltammetry and constant-potential coulometry were performed by using a PAR model 273 potentiostat. Rotating-disc voltammetry was performed by a PAR model 237 potentiostat with a Pine Instrument model ASR-2 analytical rotator and an edge-plane pyrolytic graphite electrode.

X-Ray Structure Determination of cis-$[RuL^1(Cl)(H_2O)][ClO_4]_2\cdot 2H_2O$.—*Crystal data.* The complex crystallised from aqueous CF_3CO_2H (0.1 mol dm^{-3}) as greenish brown prisms. Details of the crystal parameters, data collection, and structure refinement are given in Table 1. Raw intensities collected on a Nicolet R3m/V four-circle diffractometer at room temperature (294 K) were processed with the profile-fitting procedure of Diamond[7] and corrected for absorption using ψ-scan data.[8] The atoms comprising the RuN_4OCl co-ordination octahedron were located by direct phase determination, and the co-ordinates of the other non-hydrogen atoms were derived from successive Fourier difference syntheses. All non-hydrogen atoms except the oxygen atoms of the perchlorate group were subjected to anisotropic refinement, and the hydrogen atoms of the quadridentate ligand were generated geometrically (C–H fixed at 0.96 Å) and assigned the same isotropic thermal parameter $U = 0.08$ Å^2. The hydrogen atoms belonging to the aqua ligand and the water molecules were not included in the structure refinement.

Computations were performed with the SHELTXL-PLUS program package[9] on a DEG Micro VAX-II computer. Analytical expressions of atomic scattering factors were employed and anomalous dispersion corrections were incorporated.[10] The maxima in the last difference map all lie in the neighbourhood of two perchlorate anions and the large thermal parameters of their oxygen atoms suggest that the perchlorate groups are somewhat disordered. Tables 2 and 3 list the atomic coordinates of non-hydrogen atoms and bond lengths and angles respectively.

Additional material available from the Cambridge Crystallographic Data Centre comprises H-atom coordinates and thermal parameters.

Results and Discussion

The tetradentate ligand L^1, with its small cavity size, was found to react with $K_2[RuCl_5(H_2O)]$ to give *cis*-$[Ru^{III}L^1Cl_2]^+$ in a manner similar to the reported synthesis of *trans*-tetraaminedichlororuthenium(III) complexes.[11] The *cis* geometry was inferred from the X-ray structure of *cis*-$[Ru^{III}L^1(Cl)(H_2O)]^{2+}$. Instead of forming the desired product *cis*-$[Ru^{III}L^1(OH)(H_2O)]^{2+}$, only one chloro group of *cis*-$[Ru^{III}L^1Cl_2]^+$ was removed by Ag^I, giving *cis*-$[Ru^{III}L^1(Cl)(H_2O)]^{2+}$, the structure of which has been established by X-ray crystallography. This finding is not unreasonable in view of the X-ray result that the Ru–Cl distance in *cis*-$[Ru^{III}L^1(Cl)(H_2O)]^{2+}$ is 2.307(4) Å which is shorter than the values of 2.371(1) and 2.342(1) Å in *cis*-$[Ru^{III}L^2Cl_2]Cl$ (L^2 = cyclam = 1,4,8,11-tetraazacyclotetradecane)[12] and 2.345(4) Å in *cis*-$[Ru^{III}L^3Cl_2]ClO_4$ (L^3 = *N,N,N′N*-3,6-hexamethyl-3,6-diazaoctane-1,8-diamine)[13] respectively. Attempts have been made to isolate *cis*-$[Ru^VL^1(Cl)O]^{2+}$ through cerium(IV) oxidation of the ruthenium(III) precursor. A black solution was usually found and no well characterised product could be isolated.

The measured μ_{eff} of 1.8 μ_B for *cis*-$[Ru^{III}L^1(Cl)(H_2O)]^{2+}$ at room temperature is close to the spin-only value for one unpaired electron (Ru^{III}, $t_{2g}{}^5$). The measured pK_a value of 3.9 is slightly lower than the corresponding value of 4.1 for $[Ru^{III}(NH_3)_5(H_2O)]^{3+}$.[14]

The UV–VIS spectrum of *cis*-$[Ru^{III}L^1(Cl)(H_2O)]^{2+}$ in 0.1 mol

Table 3 Bond lengths (Å) and angles (°)

(*i*) Co-ordination geometry about Ru			
Ru–Cl(1)	2.307(4)	Ru–O(1)	2.070(9)
Ru–N(1)	2.098(10)	Ru–N(2)	2.097(10)
Ru–N(3)	2.126(10)	Ru–N(4)	2.086(10)
Cl(1)–Ru–O(1)	93.0(3)	Cl(1)–Ru–N(1)	86.9(3)
O(1)–Ru–N(1)	96.7(4)	Cl(1)–Ru–N(2)	92.7(3)
O(1)–Ru–N(2)	172.9(4)	N(1)–Ru–N(2)	79.3(4)
Cl(1)–Ru–N(3)	173.7(3)	O(1)–Ru–N(3)	90.0(4)
N(1)–Ru–N(3)	98.3(4)	N(2)–Ru–N(3)	84.8(4)
Cl(1)–Ru–N(4)	95.9(3)	O(1)–Ru–N(4)	85.4(4)
N(1)–Ru–N(4)	176.5(4)	N(2)–Ru–N(4)	98.4(4)
N(3)–Ru–N(4)	78.8(4)		
(*ii*) Ligand L^1			
N(1)–C(1)	1.32(2)	N(1)–C(5)	1.36(2)
N(2)–C(6)	1.47(2)	N(2)–C(7)	1.51(2)
N(2)–C(15)	1.48(2)	N(3)–C(8)	1.46(2)
N(3)–C(9)	1.52(2)	N(3)–C(16)	1.47(2)
N(4)–C(10)	1.33(2)	N(4)–C(14)	1.36(2)
C(1)–C(2)	1.36(2)	C(2)–C(3)	1.35(2)
C(3)–C(4)	1.40(2)	C(4)–C(5)	1.37(2)
C(5)–C(6)	1.52(2)	C(7)–C(8)	1.57(2)
C(9)–C(10)	1.50(2)	C(10)–C(11)	1.38(2)
C(11)–C(12)	1.36(3)	C(12)–C(13)	1.39(3)
C(13)–C(14)	1.40(2)		
Ru–N(1)–C(1)	127.4(9)	Ru–N(1)–C(5)	114.4(8)
C(1)–N(1)–C(5)	118(1)	Ru–N(2)–C(6)	107.1(7)
Ru–N(2)–C(7)	106.6(8)	C(6)–N(2)–C(7)	108(1)
Ru–N(2)–C(15)	114.7(8)	C(6)–N(2)–C(15)	110(1)
C(7)–N(2)–C(15)	111(1)	Ru–N(3)–C(8)	106.5(8)
Ru–N(3)–C(9)	105.6(8)	C(8)–N(3)–C(9)	109(1)
Ru–N(3)–C(16)	113.6(8)	C(8)–N(3)–C(16)	111(1)
C(9)–N(3)–C(16)	111(1)	Ru–N(4)–C(10)	116.1(9)
Ru–N(4)–C(14)	124.7(9)	C(10)–N(4)–C(14)	119(1)
N(1)–C(1)–C(2)	122(1)	C(1)–C(2)–C(3)	121(1)
C(2)–C(3)–C(4)	119(1)	C(3)–C(4)–C(5)	118(1)
N(1)–C(5)–C(4)	123(1)	N(1)–C(5)–C(6)	114(1)
C(4)–C(5)–C(6)	123(1)	N(2)–C(6)–C(5)	111(1)
N(2)–C(7)–C(8)	108(1)	N(3)–C(8)–C(7)	110(1)
N(3)–C(9)–C(10)	109(1)	N(4)–C(10)–C(9)	115(1)
N(4)–C(10)–C(11)	123(1)	C(9)–C(10)–C(11)	122(1)
C(10)–C(11)–C(12)	119(2)	C(11)–C(12)–C(13)	120(2)
C(12)–C(13)–C(14)	119(2)	N(4)–C(14)–C(13)	120(1)
(*iii*) Perchlorate ions			
Cl(2)–O(2)	1.34(3)	Cl(2)–O(3)	1.37(2)
Cl(2)–O(4)	1.35(2)	Cl(2)–O(5)	1.41(1)
Cl(3)–O(6)	1.38(3)	Cl(3)–O(7)	1.44(3)
Cl(3)–O(8)	1.39(2)	Cl(3)–O(9)	1.39(2)
O(2)–Cl(2)–O(3)	116(2)	O(2)–Cl(2)–O(4)	101(2)
O(3)–Cl(2)–O(4)	106(1)	O(2)–Cl(2)–O(5)	113(1)
O(3)–Cl(2)–O(5)	108(1)	O(4)–Cl(2)–O(5)	113(1)
O(6)–Cl(3)–O(7)	98(2)	O(6)–Cl(3)–O(8)	93(2)
O(7)–Cl(3)–O(8)	127(1)	O(6)–Cl(3)–O(9)	108(2)
O(7)–Cl(3)–O(9)	114(1)	O(8)–Cl(3)–O(9)	112(1)
(*iv*) Hydrogen bonding			
O(1) ··· O(10)	2.62(2)	O(1) ··· O(11)	2.63(2)
O(10) ··· Cl(1a)	3.23(1)	O(10) ··· O(4b)	2.91(2)
O(11) ··· O(5b)	2.91(2)	O(11) ··· O(9c)	2.86(2)
Ru–O(1) ··· O(10)	127(1)	Ru–O(1) ··· O(11)	118(1)
O(10) ··· O(1) ··· O(11)	99(1)	Cl(1a) ··· O(10) ··· O(1)	137(1)
Cl(1a) ··· O(10) ··· O(4b)	125(1)	O(1) ··· O(10) ··· O(4b)	94(1)
O(1) ··· O(11) ··· O(5b)	107(1)	O(1) ··· O(11) ··· O(9c)	106(1)
O(5b) ··· O(11) ··· O(9c)	94(1)		

Symmetry transformations: a $-\frac{1}{2} + x, y, \frac{1}{2} - z$; b $-\frac{1}{2} + x, \frac{1}{2} - y, 1 - z$; c $\frac{1}{2} + x, \frac{1}{2} - y, 1 - z$

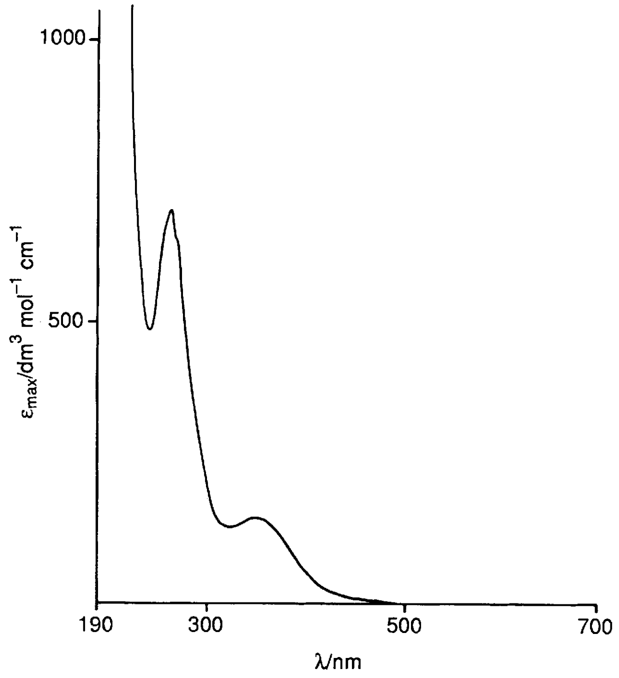

Fig. 1 The UV-VIS spectrum of *cis*-$[Ru^{III}L^1(Cl)(H_2O)]^{2+}$ in 0.1 mol dm^{-3} CF_3CO_2H

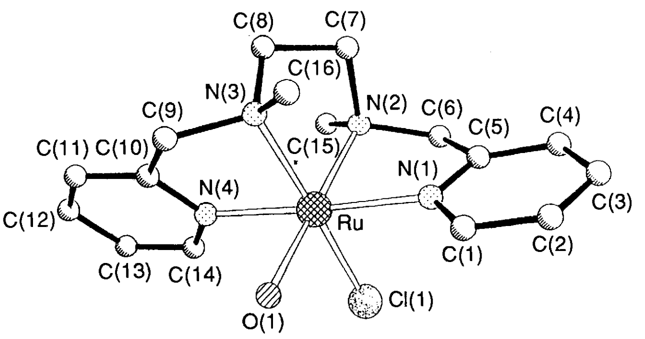

Fig. 2 An ORTEP plot of *cis*-$[Ru^{III}L^1(Cl)(H_2O)]^{2+}$

dm^{-3} CF_3CO_2H is shown in Fig. 1. It is featureless and dominated by the intraligand transitions.

Structure Description of *cis*-$[Ru^{III}L^1(Cl)(H_2O)][ClO_4]_2 \cdot 2H_2O$.—A perspective view of the *cis*-$[Ru^{III}L^1(Cl)(H_2O)]^{2+}$ cation is shown in Fig. 2 with the atom numbering. The Ru^{III} is in an octahedral co-ordination environment with two unidentate ligands, Cl^- and H_2O, *cis* to each other and two pyridyl groups occupying *trans* positions. The Ru–N distances are normal and span a narrow range [2.13(1)–2.09(1) Å]. The Ru–OH_2 distance of 2.070(9) Å is longer than the values in $[Ru^{III}(H_2O)_6]^{3+}$ [2.016(4)–2.037(5) Å][15] and *trans*-$[Ru^{III}(bipy)_2(OH)(H_2O)]^{2+}$ (bipy = 2,2′-bipyridyl) [2.007(3) Å],[16] but shorter than those in $[Ru^{III}L^4(H_2O)]^{2+}$ {HL^4 = bis[2-(2-pyridyl)ethyl][2-hydroxy-2-(2-pyridyl)ethyl]amine [2.115(3) Å][3c] and $[\{Ru(bipy)_2(H_2O)\}_2O]^{4+}$ [2.136(4) Å].[2b] The variation in Ru–OH_2 distances in these ruthenium(III) complexes could be due to the difference in the d_π(Ru) and $p_\pi(OH_2)$ interaction, which is affected by the donor atom *trans* to the aqua ligand. The Ru–Cl bond of 2.307(4) Å is significantly shorter than those in *cis*-$[Ru^{III}(cyclam)(Cl_2)]^+$ [2.371(1) Å][12] and *cis*-$[Ru^{III}L^3Cl_2]^+$ [2.345(4) Å].[13]

In octahedral metal complexes the linear quadridentate amine ligands fully N-bonded to the central metal atom potentially provide a diversity of possible geometrical and configurational isomers.[17] According to the wrapping mode of such a ligand about the metal centre, there are three possible conformations, *trans*, *cis*-α and *cis*-β for complexes with the

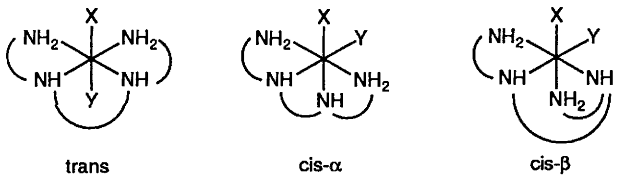

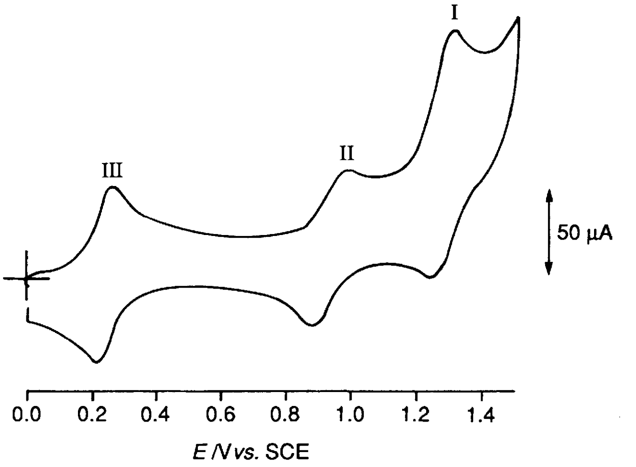

Fig. 3 Cyclic voltammogram of *cis*-$[Ru^{III}L^1(Cl)(H_2O)]^{2+}$ in 0.1 mol dm^{-3} CF_3CO_2H. Working electrode: edge-plane pyrolytic graphite. Scan rate: 50 mV s^{-1}

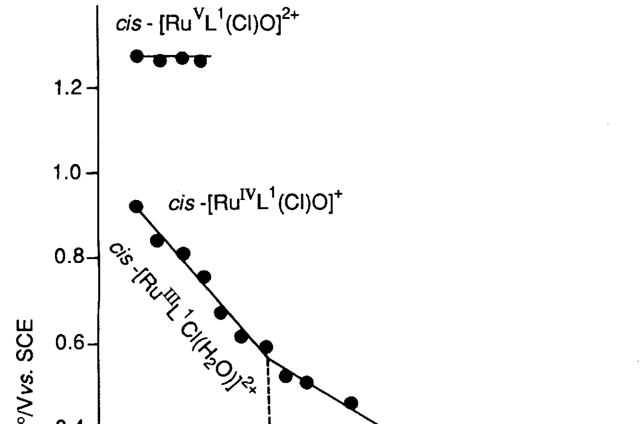

Fig. 4 Pourbaix diagram of *cis*-$[Ru^{III}L^1(Cl)(H_2O)]^{2+}$ at different pH values. Conditions as in Fig. 3

Table 4 Summary of E° values for various redox couples of *cis*-$[Ru^{III}L^1Cl(H_2O)]^{2+}$ at different pH and 25 °C. Working electrode: edge-plane pyrolytic graphite

	E°/V *vs.* SCE		
pH	Couple I	Couple II	Couple III
1.0	1.29	0.92	0.23
1.5	1.28	0.85	0.23
2.0	1.28	0.81	0.24
2.5	1.28	0.76	0.23
3.0		0.69	0.23
3.5		0.63	0.21
4.0		0.59	0.20
4.5		0.54	0.18
5.0		0.51	0.16
6.0		0.46	0.12
7.0		0.39	0.05
8.0		0.35	0.01
9.0		0.28	−0.06
10.0		0.21	−0.12

general formula ML(X)Y where X or Y is a unidentate ligand and L is a quadridentate amine ligand. In addition, there are several isomeric possibilities related to the configurations of the two inner nitrogen atoms in each conformational isomer. Sargeson and Searle's systematic study of the Co^{III}–trien [trien = $NH_2(CH_2)_2NH(CH_2)_2NH(CH_2)_2NH_2$] system[18] showed that in most circumstances trien has a tendency to form *cis*-[Co(trien)X(Y)] complexes, and the relative stability of the α and β isomer is influenced by the unidentate ligands X and Y rather than the strain associated with co-ordination of the secondary N atoms in the two configurations. Another study[19] on the transition metal–$NH_2(CH_2)_3NH(CH_2)_2NH(CH_2)_3NH_2$ system showed that amine co-ordination tends to produce *trans* complexes. In the present work, the bulky, rigid pyridinyl group at both ends of the ligand renders it difficult to form *trans* and *cis*-β isomers with the Ru^{III}, so that the only product obtained is the *cis*-α isomer.

Electrochemistry.—The cyclic voltammogram of *cis*-$[Ru^{III}L^1(Cl)(H_2O)]^{2+}$ in 0.1 mol dm^{-1} CF_3CO_2H (pH 1.1) with an edge-plane pyrolytic graphite electrode is shown in Fig. 3. Three reversible/quasi-reversible couples I–III were observed at 1.29, 0.93 and 0.23 V *vs.* saturated calomel electrode (SCE) respectively. Constant-potential coulometry at 0.15 and 1.0 V *vs.* SCE established that n = 1.0 for couples II and III. Couples II and III are thus assigned to be Ru^{IV}–Ru^{III} and Ru^{III}–Ru^{II} respectively. Constant-potential electrolysis at 1.3 V, however, was found to lead to a non-stop counting of the coulombs passed. It is likely that the potential held was too close to the anodic limit of the electrolyte system and hence some solvent decomposition was occurring at this potential. On the other hand, slow decomposition of the complex may also have occurred. Rotating-disc voltammetry, however, showed that the plateau currents for couples I–III are all similar in magnitude. Hence it is reasonable to assign couple I to be the one-electron couple Ru^V–Ru^{IV}.

It is interesting that the couple Ru^{III}–Ru^{II} is reversible, in contrast to what is found for other chlororuthenium(III) amine systems.[20] In previous work, electrogenerated *trans*- or *cis*-dichlororuthenium(II) complexes were found to undergo rapid solvolysis, $Ru^{II}\text{–}Cl + H_2O \longrightarrow Ru^{II}\text{–}OH_2 + Cl^-$ on the time-scale of cyclic voltammetric scans. The present result indicates that the chloride ligand in *cis*-$[Ru^{II}L^1(Cl)(H_2O)]^+$ is not so reactive towards solvolysis and remains intact on this time-scale.

The Pourbaix diagram over the range pH 1–10 is shown in Fig. 4 and the electrochemical data are summarised in Table 4. Couple I is independent of pH and is assigned to reaction (1).

$$cis\text{-}[Ru^VL^1(Cl)O]^{2+} + e^- \longrightarrow cis\text{-}[Ru^{IV}L^1(Cl)O]^+ \quad (1)$$

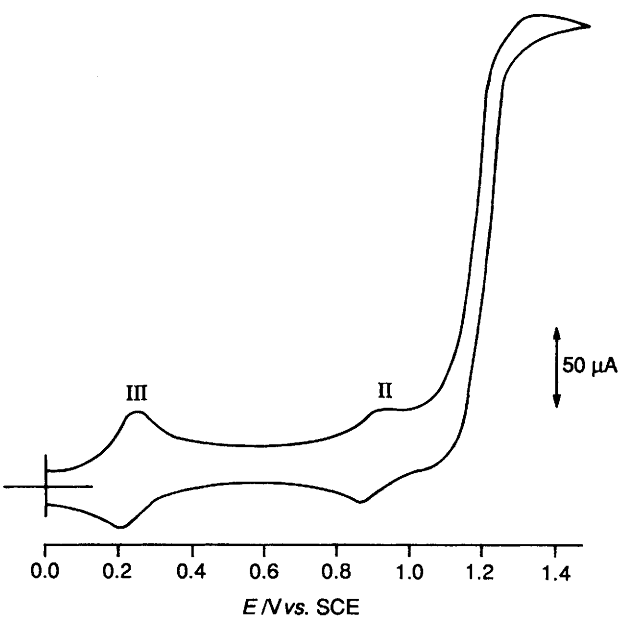

Fig. 5 Cyclic voltammogram of 1 mmol dm^{-3} *cis*-$[Ru^{III}L^1(Cl)(H_2O)]^{2+}$ in the presence of 10 mmol dm^{-3} benzyl alcohol in 0.1 mol dm^{-3} CF_3CO_2H. Conditions as in Fig. 3

Table 5 Results of constant-potential electrocatalytic oxidation of organic substrates by *cis*-$[Ru^VL^1(Cl)O]^{2+}$. Reaction time: 8 h

Substrate	Product	Current efficiency (%)	Turnover
Tetrahydrofuran	γ-Lactone	84	23
Propan-2-ol	Acetone	92	40
Methanol	Formaldehyde	87	28
Ethanol	Acetaldehyde	95	36
Cyclobutanol	Cyclobutanone	93	30
Benzyl alcohol	Benzaldehyde	95	38

At pH > 2.5, the couple Ru^{IV}–Ru^V is masked by the solvent oxidation peak and hence its E° could not be measured.

For couple II two straight-line segments with slopes of −118 ($1.1 < pH < 4.1$) and −60 mV per pH unit (pH > 4.1) are found. On the basis of this result the electrode reactions are (2) and (3) respectively.

$$cis\text{-}[Ru^{IV}L^1(Cl)O]^+ + 2H^+ + e^- \longrightarrow cis\text{-}[Ru^{III}L^1(Cl)H_2O)]^{2+} \quad (2)$$

$$cis\text{-}[Ru^{IV}L^1(Cl)O]^+ + H^+ + e^- \longrightarrow cis\text{-}[Ru^{III}L^1(Cl)(OH)]^+ \quad (3)$$

Couple III is independent of pH for $1.1 < pH < 4.1$, but at pH > 4.1, a slope of −58 mV per pH unit was obtained. The corresponding electrode reactions are (4) and (5) respectively.

$$cis\text{-}[Ru^{III}L^1(Cl)(H_2O)]^{2+} + e^- \longrightarrow cis\text{-}[Ru^{II}L^1(Cl)(H_2O)]^+ \quad (4)$$

$$cis\text{-}[Ru^{III}L^1(Cl)(OH)]^+ + H^+ + e^- \longrightarrow cis\text{-}[Ru^{II}L^1(Cl)(H_2O)]^+ \quad (5)$$

The break-point of the plot for couple III occurs at pH 4.1 which is the pK_a value of *cis*-$[Ru^{III}L^1(Cl)(H_2O)]^{2+}$. The value is close to that of 3.9 ± 0.3 determined by spectrophotometry.

The cyclic voltammogram of *cis*-$[Ru^{III}L^1(Cl)(H_2O)]^{2+}$ in the presence of benzyl alcohol is shown in Fig. 5. Couples II and III remain unchanged while couple I is replaced by a large catalytic oxidative wave at *ca.* 1.2 V *vs.* SCE. The large oxidative wave can be explained by rapid oxidation of benzyl alcohol by electrogenerated *cis*-$[Ru^VL^1(Cl)O]^{2+}$ which is reduced back to Ru^{IV} or Ru^{III}. Similar results have been observed with other alcohols and tetrahydrofuran.

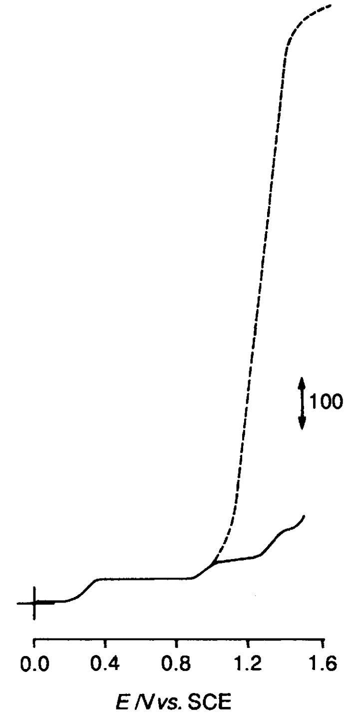

Fig. 6 Rotating-disc voltammogram of 1 mmol dm^{-3} *cis*-$[Ru^{III}L^1(Cl)(H_2O)]^{2+}$ (——) and in the presence of 10 mmol dm^{-3} benzyl alcohol (– – – –). Supporting electrolyte: 0.1 mol dm^{-3} CF_3CO_2H. Working electrode: edge-plane pyrolytic graphite. Scan rate: 5 mV s^{-1}

The results for the electrochemical oxidation of different organic substrates at a potential of 1.1 V mediated by *cis*-$[Ru^{III}L^1(Cl)(H_2O)]^{2+}$ are summarised in Table 5. A current efficiency over 85% was found in each case. After electrolysis for 8 h over 80% of *cis*-$[Ru^{III}L^1(Cl)(H_2O)]^{2+}$ was recovered as determined by UV-VIS spectrophotometry. Thus the present catalyst is superior to *trans*-$[Ru^{III}(phen)(OH)(H_2O)]^{2+}$ (phen = 1,10-phenanthroline)[21] and $[Ru^{IV}(terpy)(bipy)O]^{2+}$ (terpy = 2,2′:6′,2″-terpyridyl)[22] systems, in which cases the catalysts turned to a green species upon extended electrolysis.

Levich plots of i_L (plateau current) *vs* $\omega^{\frac{1}{2}}$ (ω = rotation rate) for the couples Ru^{III}–Ru^{II}, Ru^{IV}–Ru^{III} and Ru^V–Ru^{IV} in 0.1 mol dm^{-3} CF_3CO_2H are straight lines that pass through the origin. The plot for Ru^{IV}–Ru^{III} showed a negative deviation from the straight line at ω > 2500 revolutions min^{-1} and this may be due to the deprotonation step in the formation of the ruthenium oxo from the ruthenium aqua complex. The diffusion coefficient for *cis*-$[Ru^{III}L^1(Cl)(H_2O)]^{2+}$ was calculated from the slope to be 4.98×10^{-6} cm^2 s^{-1}.

A large catalytic current was observed when benzyl alcohol was added to the solution (Fig. 6). In the presence of an excess of benzyl alcohol the plateau current at 1.4 V becomes less and less dependent on the rotation rate of the electrode. This is expected because in the presence of a large excess of benzyl alcohol the electrogenerated Ru^V=O species only consumes a very small amount of benzyl alcohol but the rate of oxidation is rapid enough to establish a stationary concentration of catalyst at the electrode surface. Under such conditions, limiting currents independent of scan rates are expected. The electrochemical data can be used to calculate the rate constant for the homogeneous cross-reaction between the substrate and catalyst if a simple pseudo-first-order reaction is assumed [equation (6)][23]

$$i_{cat} = nFAC_RD_R^{\frac{1}{2}}k^{\frac{1}{2}}C_s^{\frac{1}{2}} \quad (6)$$

Table 6 Comparison of second-order rate constants for oxidation of benzyl alcohol by some ruthenium oxo complexes

Catalyst	E°/V *vs.* NHE	Medium	k/dm^3 mol^{-1} s^{-1}
cis-$[\mathrm{Ru^VL^1(Cl)O}]^{2+}$	1.53	0.1 mol dm^{-3} CF_3CO_2H	8.4×10^4
trans-$[\mathrm{Ru^VL^5(Cl)O}]^{2+}$ [3a]	1.45	0.1 mol dm^{-3} NEt_4BF_4–MeCN	2.1×10^2
trans-$[\mathrm{Ru^VL^5(NCO)O}]^{2+}$ [3a]	1.29	0.1 mol dm^{-3} NEt_4BF_4–MeCN	1.4×10^2
$[\mathrm{Ru^VL^4(O)}]^{2+}$ [3d]	1.24	0.1 mol dm^{-3} CF_3CO_2H	1.2×10^2

where i_{cat} is the limiting current, F is the Faraday constant, C_s is the substrate concentration, C_R and D_R are the catalyst concentration and diffusion coefficient respectively, and k is the second-order rate constant. At 0.5 mmol dm^{-3} *cis*-$[\mathrm{Ru^{III}L^1(Cl)(H_2O)}]^{2+}$ and 20 mmol dm^{-3} benzyl alcohol, the experimental limiting currents were almost independent of rotation rate. The rate constant for the reaction between *cis*-$[\mathrm{Ru^VL^1(Cl)O}]^{2+}$ and benzyl alcohol was calculated from equation (6) at a rotation rate of 400 revolutions min^{-1} as 8.4×10^4 dm^3 mol^{-1} s^{-1}. Thus *cis*-$[\mathrm{Ru^VL^1(Cl)O}]^{2+}$ is a much more reactive oxidant than *trans*-$[\mathrm{Ru^VL^5(Cl)O}]^{2+}$ (L^5 = 1,4,8,11-tetramethyl-1,4,8,11-tetraazacyclotetradecane)[3a] or $[\mathrm{Ru^VL^4(O)}]^{2+}$.[3c,d] A comparison of the second-order rate constants for the oxidation of benzyl alcohol by some ruthenium oxo complexes is shown in Table 6. While the high reactivity of *cis*-$[\mathrm{Ru^VL^1(Cl)O}]^{2+}$ can be partly attributed to the high potential of the couple $\mathrm{Ru^V}$–$\mathrm{Ru^{IV}}$, the fact that the rates of oxidation do not correlate linearly with the E° values of the $\mathrm{Ru^V{=}O}$ oxidants argues that the reaction is not just governed by the charge transfer from the alcohol to the $\mathrm{Ru^V{=}O}$ moiety. Previous studies have shown that oxidation of alcohols by ruthenium oxo complexes involves the hydrogen atom or hydride abstraction as the rate-determining step.[3d,24] It is likely that the present $\mathrm{Ru^V{=}O}$ species may react by a similar mechanism.

Conclusion

The newly synthesised *cis*-$[\mathrm{Ru^{III}L^1(Cl)(H_2O)}]^{2+}$ has been found to be a good precursor for the generation of monooxoruthenium(V). Having a E° value of 1.29 V (*vs.* SCE), *cis*-$[\mathrm{Ru^VL^1(Cl)O}]^{2+}$ is capable of oxidising alcohols at a rate superior than those of reported $\mathrm{Ru^V{=}O}$ species. High current efficiency and turnovers for the electrochemical oxidation of alcohols and tetrahydrofuran mediated by the couple $\mathrm{Ru^V}$–$\mathrm{Ru^{IV}}$ were found. The present findings suggest that $\mathrm{Ru^V{=}O}$ complexes, if suitably designed, have potential application in electrochemical oxidation of alkanes.

Acknowledgements

We acknowledge support from the University of Hong Kong and the University and Polytechnic Granting Committee (UPGC).

References

1 W. P. Griffith, *Transition Met. Chem.*, 1990, **15**, 251.

2 (*a*) F. P. Rotzinger, S. Munavalli, P. Comte, J. K. Hurst, M. Gratzel, F. J. Pern and A. J. Frank, *J. Am. Chem. Soc.*, 1987, **109**, 6619; (*b*) J. A. Gilbert, D. S. Eggleston, W. R. Murphy, jun., D. A. Geselowitz, S. W. Gersten, D. J. Hodgson and T. J. Meyer, *J. Am. Chem. Soc.*, 1985, **107**, 855.

3 (*a*) K. Y. Wong, C. M. Che and F. C. Anson, *Inorg. Chem.*, 1987, **26**, 737; (*b*) C. M. Che and K. Y. Wong, *J. Chem. Soc., Chem. Commun.*, 1986, 229; (*c*) C. M. Che, V. W. M. Yam and T. C. W. Mak, *J. Am. Chem. Soc.*, 1990, **112**, 2284; (*d*) C. M. Che, C. Ho and T. C. Lau, *J. Chem. Soc., Dalton Trans.*, preceding paper.

4 A. C. Dengel, W. P. Griffith, C. A. O'Mahoney and D. J. Williams, *J. Chem. Soc., Chem. Commun.*, 1989, 1720.

5 See, for example, C. M. Che, T. F. Lai and K. Y. Wong, *Inorg. Chem.*, 1987, **26**, 2289.

6 C. M. Che, W. T. Tang, W. T. Wong, K. Y. Wong and T. F. Lai, *J. Chem. Res.* (*s*), 1991, 30.

7 R. Diamond, *Acta Crystallogr., Sect. A*, 1969, **25**, 43.

8 G. Kopfmann and R. Hubber, *Acta Crystallogr., Sect A*, 1968, **24**, 348.

9 G. M. Sheldrick, in *Crystallographic Computing 3. Data Collection, Structure Determination, Proteins and Databases* eds. G. M. Sheldrick, C. Kruger and R. Goddard, Oxford University Press, New York, 1985, p. 175.

10 *International Tables for X-Ray Crystallography*, Kynoch Press, Birmingham, 1974, vol. 4, pp. 55, 99, 149.

11 C. K. Poon and C. M. Che, *J. Chem. Soc., Dalton Trans.*, 1980, 756; C. M. Che, S. S. Kwong and C. K. Poon, *Inorg. Chem.*, 1985, **24**, 1601.

12 C. M. Che, S. S. Kwong, C. K. Poon, T. F. Lai and T. C. W. Mak, *Inorg. Chem.*, 1985, **24**, 1359.

13 C. M. Che, W. T. Tang, M. H. W. Lam and T. C. W. Mak, *J. Chem. Soc., Dalton Trans.*, 1988, 2885.

14 C. G. Kuehn and Taube, *J. Am. Chem. Soc.*, 1976, **98**, 689.

15 V. Dong, H. J. Keller, H. Endres, W. Moroni and D. Nothe, *Acta Crystallogr., Sect. B*, 1977, **33**, 2428.

16 B. Durham, S. R. Wilson, D. J. Hodgson and T. J. Meyer, *J. Am. Chem. Soc.*, 1980, **102**, 600.

17 D. A. House in *Comprehensive Coordination Chemistry*, vol 2, eds. G. Wilkinson, R. D. Gillard and J. A. McCleverty, Pergamon, New York, 1987, p. 23.

18 A. M. Sargeson and G. H. Searle, *Inorg. Chem.*, 1967, **4**, 787.

19 B. Bosnich, J. M. Harrowfield and H. Boncher, *Inorg. Chem.*, 1975, **14**, 815.

20 C. K. Poon, C. M. Che and Y. P. Kan, *J. Chem. Soc., Dalton Trans.*, 1980, 128.

21 C. M. Che, W. H. Leung and C. K. Poon, *J. Chem. Soc., Chem. Commun.*, 1987, 173.

22 M. S. Thompson, W. F. deGiovani, B. A. Moyer and T. J. Meyer, *J. Org. Chem.*, 1984, **49**, 4972.

23 Z. Galus, *Fundamentals of Electrochemical Analysis*, Halsted Press, New York, 1976, p. 375.

24 L. Roecker and T. J. Meyer, *J. Am. Chem. Soc.*, 1987, **109**, 746.

Received 7*th January* 1991; *Paper* 1/00086A